

NUMERICAL MODELLING OF FASTNET LIGHTHOUSE BASED ON EXPERIMENTAL DYNAMIC IDENTIFICATION

A. Pappas⁽¹⁾, D. D'Ayala⁽¹⁾, A. Antonini⁽²⁾, J. Brownjohn⁽³⁾ and A. Raby⁽²⁾

(1) University College London, UK

(2) Plymouth University, UK

(3) University of Exeter, UK

Abstract

The Fastnet Lighthouse is an impressive seamark on a small islet in the Atlantic Ocean and the most southerly point of Ireland. It has been guiding mariners in their perilous profession since 1904. Its importance to the safety of navigation, in combination with its heritage value and reported vibrations, led to the structural analysis of this iconic monument.

Accessing the lighthouse by helicopter, experimental dynamic identification and material characterisation was performed. A detailed finite element model was built based on original archival drawings representing the built state. The commercial software Abaqus was used for the finite element modelling. The initial numerical properties of the model were assigned based on bibliographic research on the original materials. The calibration of the numerical model was based on the on-site material characterisation results and modal testing. A parametric analysis was also performed for identifying the influence of parameters such as the modulus of elasticity, weight of the lighting apparatus and type of foundations to the numerical modal analysis results.

This work is part of the STORMLAMP project (SStructural behaviour Of Rock Mounted Lighthouses At the Mercy of imPulsive waves) funded by the UK Engineering and Physical Sciences Research Council.

1. INTRODUCTION

Fastnet Lighthouse lies 13km from the southernmost mainland point of Ireland and 6.5km southwest of Cape Clear island. The construction of this stunning monument was a very demanding challenge that began in 1897 and finished 7 years later. Construction work was suspended during winter months due to extreme weather conditions and high waves. This new granite lighthouse, designed by William Douglass for replacing an existing and insufficient cast iron lighthouse of 1854, started operating the night of 16 June 1904.

Valuable information about the geometry and construction typology was obtained by very detailed original drawings provided by the Irish Lights, a body that serves as the General Lighthouse Authority for Ireland plus its adjacent seas and islands. The lighthouse consists of a 36.7m high tapered masonry body and an 8.3m high lantern which houses the lighting apparatus (Figure 1). The diameter is 12.10m at the base and gradually decreases to 6.25m near the top. The first 12 courses, i.e. up to the height of 6.62m, consist of solid masonry without inner openings. A substructure of 13 incomplete courses lies below these first complete courses as its base is built into the rock. The masonry structure comprises 8 different levels divided by vaulted floors, plus the lantern structure on the top. The wall thickness varies between 2.44m

at the entrance level and 0.76m at the upper level. Each block is connected to the next with elaborate dovetailed joggles. This results in a very solid and bonded structural system that does not allow sliding between blocks unless the dovetailed joggles are broken. Moreover, the joints between stones are filled with fine cement mortar. A total of 2074 granite blocks, with a weight of 4300 tonnes were required for the construction [1].

The granite for the construction of the tower was purchased from John Freeman & Sons of Penryn, Cornwall [1]. Thanks to a descriptive catalogue of 1911 [2], it was found that John Freeman & Sons traded a light grey, coarse-grained, porphyritic muscovite biotite granite with a density of 2643 kg/m^3 .

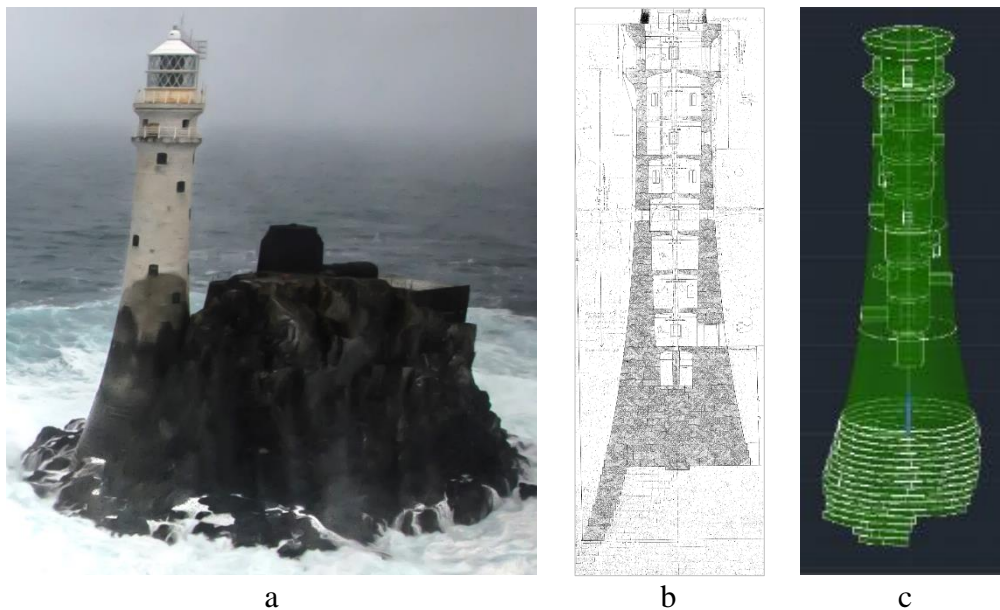


Figure 1: (a) Aerial view of Fastnet Rock; (b) original drawings of Fastnet lighthouse provided by the Irish Lights; (c) CAD model.

2. FINITE ELEMENT MODEL

The finite element numerical model of Fastnet lighthouse was created with the commercial software Abaqus 6.14 (2014). A structured and swept mesh with hexahedral elements was used for the greatest part of the model. A maximum finite element size of 0.25 m with a further refinement of 0.20 m near the openings was adopted. Homogeneous isotropic material properties were assigned to the model. Non-structural masses were added on the top stone course of the structure for simulating the mass of the lantern with the lighting apparatus and the mercury-filled circular cast-iron pedestal support (Figure 2). The weight of the rotating device itself is estimated around 6 tonnes [1].

The broadening of the area that was used as the base of the main structure was modelled in detail (Figure 3). Due to the complexity of the geometry, tetrahedral finite elements were used for meshing this area. Including the substructure, the total mass of the model (without the added mass at the top) was 4382 tonnes. This differs by less than 3.6% from the estimation of 4300 imperial tons (i.e. 4232 tonnes) of granite used for the construction [1]. This very good correlation, in combination with the detailed archival drawings, validate the geometry of the model and the assigned material density.

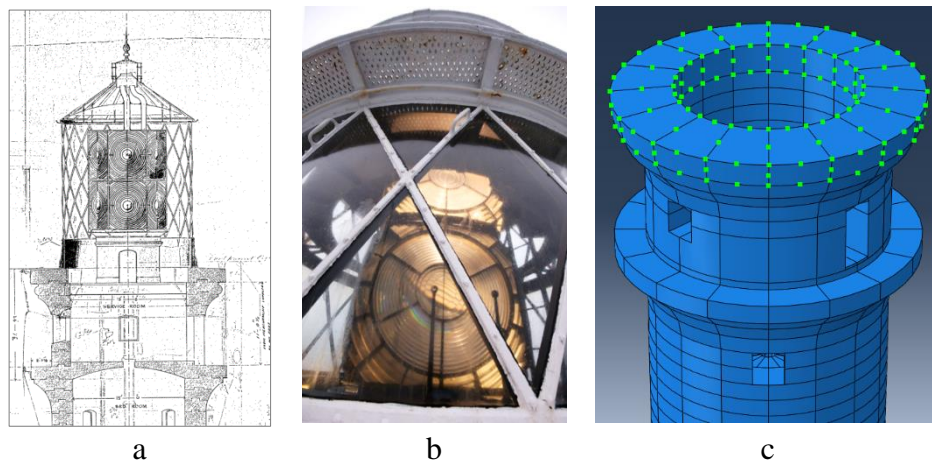


Figure 2: Lighting apparatus room: (a) archival drawing; (b) on-site photograph; (c) non-structural mass distributed on the upper course of blocks of the FE model.

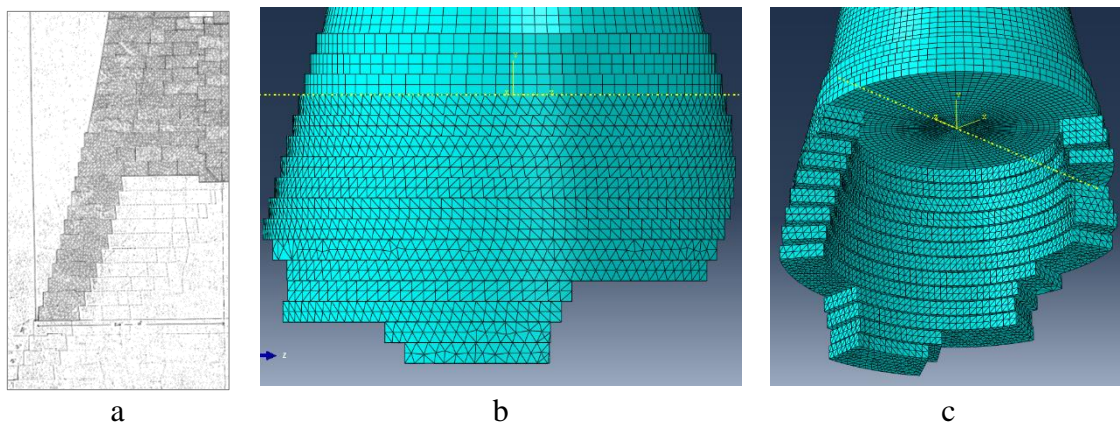


Figure 3: Substructure: (a) archival drawing; (b) frontal view of the meshed model; (c) bottom view of the meshed model

3. DYNAMIC IDENTIFICATION TESTING

A field campaign on an offshore lighthouse requires a high degree of planning. The main restrictions are related to the lifting capacity of the helicopter and to the safe weights that should be handled while moving equipment between helicopter, helipad and the lighthouse lower levels. The most relevant issue to solve is the need for a mechanical shaker, with a weight (including the amplifier and the required cables) exceeds 80 kg.

The ideal monitoring solution of monitoring in both directions, was impeded by limited space and weight, thus the number of accelerometers was kept to a minimum.

All 9 levels were instrumented with an accelerometer except the level where the shaker was located (i.e. the kitchen at level 8), which was equipped with both x-y accelerometers. The x and y directions were identified at the same circumferential points at each level according to Irish Lights drawings showing the internal layout. The principal directions were later identified by composing and rotating both the signals recorded at the kitchen level (Figure 4).

From previous studies [4], the aim of the field modal tests was to identify the fundamental vibration modes expected to occur around 5 Hz, as well as a few higher modes sufficient to validate the numerical models.

Despite the massive structure of Fastnet lighthouse and the relatively low power of the shaker, the signal to noise ratio was adequate for estimation of the first mode. Modal masses for unit modal ordinate at level 8, the top of the masonry structure were obtained using forced vibration testing through the H1 frequency response function (FRF) estimator, while the modal shapes were identified from ambient records.

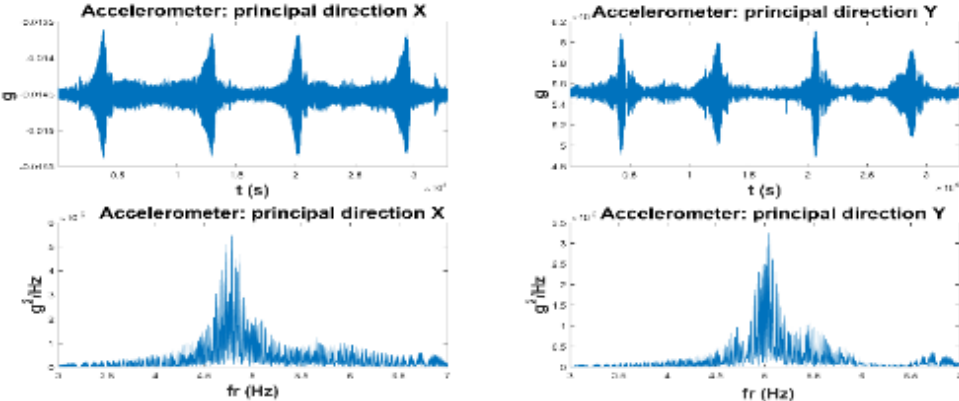


Figure 4: Principal direction time histories from the kitchen level and related power spectrum (upper panel); spectrogram from the accelerometers and shaker action (lower panel).

The best quality modal identification was obtained by single input single output (SISO) circle fitting. Figure 5, presents the circle fit of the 4.78 and 5.02 Hz modes for x and y principal directions respectively. Modal mass estimates are 242 (x direction) and 1145 (y direction) tonnes. Mode frequencies and shapes identified from ambient data using eigensystem realisation algorithm (ERA) were used for numerical model calibration, with the first 4 modes shown in Figure 7 (left). Frequencies differ slightly from the SISO values.

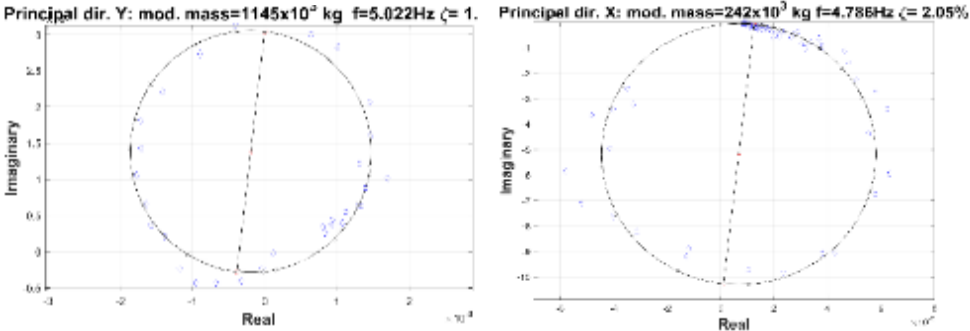


Figure 5: SISO circle fit for both principal directions.

4. SCHMIDT HAMMER TESTING

Schmidt hammer testing was performed with the use of an N-type (impact energy = 2.207 Nm) rebound hammer in order to determine the mechanical properties of the granite blocks. The tests were carried out at 6 positions on the internal side of the three lower levels of the lighthouse. These areas were selected because they were uncoated and easily accessible. Matrixes of 21 cm x 28 cm with 7 cm distance between the impact points were considered, resulting in 20 impacts per test. Only horizontal impacts were performed. In addition, 4 points were tested with 5 subsequent impacts for assessing the weathering grade of the surface.

Katz *et al.* [5] proposed Eqs.1 and 2 for predicting the Young's modulus of elasticity (E) and compressive strength (f_c) for different types of stones based on the upper 50% rebound values. However, these formulae were developed based on impact tests on dried specimens with polished surfaces. In the Fastnet on-site testing, the coarse grained granite has a slightly weathered surface and high moisture because of the humid sea air and the surficial oil condensation from the adjacent lighthouse engines. These parameters are expected to reduce the rebound level of impact [6]. However, there are no guidelines for quantifying the influence of moisture on the rebound level. Empirical graphs regarding the influence of the moisture content and weathering were proposed by Aydin and Basu [7].

$$E = 0.00013x^{3.09074} \quad (1)$$

$$f_c = 2.208e^{0.067x} \quad (2)$$

The presence of a non-smooth surface that decreases the rebound has been inferred from the difference of rebound value between the first two impacts ($R_1 - R_2$) carried out at the same point [7]. In order to use this same approach, 4 different points were tested with 5 subsequent impacts each. The results yielded an average difference between the two first impacts $R_1 - R_2 = 3.25$ which corresponds to weathering grade I-II.

Having an average rebound of 58.5, with the use of Eq.1, the Young's modulus of elasticity is calculated equal to $E = 37.65$ GPa. Based on Eq.2, the uniaxial strength is estimated equal to $f_c = 111.23$ MPa. These results correspond to the 59% and 76% of the bibliographically estimated E and f_c respectively.

As mentioned above, the value of rebound is influenced by the surficial humidity and weathering. Therefore, increased rebound values by 5% to 15%, i.e. 61.4 to 67.3, for equivalent intact, polished and dry specimens of granite is a plausible assumption. These increased rebound values would result in E values between 43.77 GPa and 57.99 GPa. Similarly, f_c is calculated between 135.31 MPa and 200.24 MPa. Compared to the bibliographic values, these results correspond 69% - 91% for E and 92% - 136% for f_c .

5. PARAMETRIC ANALYSIS

The scope of this analysis was to identify the most influential parameters to the structural response of the numerical model in terms of modal analysis. The analysed parameters were the (i) type of finite element, (ii) detail of simulation of the granite blocks below the first full courses, (iii) Young's modulus of elasticity E and (iv) amount of added mass on the upper part (Table 1). The analysis results are measured in terms of modal frequencies, direction of oscillation with respect to floor plan and effective masses (i.e. the amount of excited mass associated with a kinematic direction for each mode)

Table 1: Analysed parameters

PARAMETER	RANGE
Type of finite elements	C3D20, C3D20R, C3D8, C3D8R
Modelling the substructure	Model with substructure, model without substructure
Young's modulus of elasticity	20 GPa - 63.79 GPa
Non-structural mass	0 kg, 10000 kg, 15000 kg, 20000 kg, 25000 kg

5.1 Quadratic brick finite elements

The first parameter was the type of finite elements. Four types of brick elements of different complexity and precision were considered (Table 2). The 20-node quadratic brick elements are more precise than the 8-node elements, especially for bending problems, but at the same time the most expensive in terms of computational cost. Reduced integration can reduce slightly the computational cost, therefore reduced integration 20-node and 8-node elements were also analysed. The tests on the influence of the brick elements were run on the numerical model for an E value equal to 63.79 GPa, no added mass and without modelling the lower granite substructure.

Table 2: Brick elements used in the parametrical analysis

Element	Description
C3D20	20-node quadratic brick
C3D20R	20-node quadratic brick, reduced integration
C3D8	8-node quadratic brick
C3D8R	8-node quadratic brick, reduced integration

The results revealed very small discrepancies when compared with measured results for the first 14 modal frequency values between C3D20 and C3D20R while the difference between C3D20 and C3D8 and C3D8R was slightly higher but still not significant. The first 14 modes activated around 72% of the total mass in the two horizontal directions (X and Z) and around 66% in the vertical direction (Y). The results of C3D20 and C3D20R were very close, with less than 1% difference for all modal components with effective mass more than 5% of the total structure mass. For the same modal components, the maximum difference between the C3D20 results and the C3D3 and C3D8R becomes 5.82% and 3.41% respectively.

Summarising, the results yielded very minor differences in terms of modal frequency values (between -0.20% and 0.20% for the first 4 modes, Table 3), moderate differences in terms of effective masses (between -3.27% and 5.82% for the first 4 modes, Table 3) and major differences in terms of computational cost between the 20-node and 8-node brick elements. Therefore, although the 20-node brick element C3D20 is the most accurate, for the sake of reducing the computational demands, the parametric analysis was carried out with the 8-node brick element C3D8.

5.2 Substructure

It is obvious that modelling the substructure will influence the modal results of the structure. It was determined that the volume of deformable material under the base of the structure slightly decreased the modal frequency values. This decrease was between -0.40% and -0.98% for the first 4 modes of vibration for tested values of E between 20 GPa and 63.79 GPa (Figure 6).

Moreover, the lack of symmetry of this substructure volume in relation to the vibration axes of the main modal shapes caused a slight rotation of the direction of the modal shapes with respect to the floor plan. Variable φ is the angle between the direction of oscillation (for the flexural modal shapes) and axis X, where positive φ values indicate clockwise rotation. The results yield a difference between 3.45° and 4.18° in the direction of modal shapes between the models with and without substructure.

The mass of the substructure volume is calculated to be around 573 tonnes, approximately 13% of the total mass of the structure. Inevitably, this mass has an important contribution to the

distribution of effective masses (m^*) attributed to each mode. For the first 4 modes, the variation due to the substructure was proved to be between -21.2% and 17.1% (Table 3)

5.3 Young's modulus of elasticity

An intact granite of this type would have a high Young's modulus of elasticity around 63.79 GPa [8]. However, since the lighthouse is not an intact granite body but a structure comprising separate granite blocks, an equivalent modulus of elasticity has to be assumed. According to numerical findings, for a fractured rock body with orthogonal sets of fractures, the equivalent modulus of elasticity can be estimated around 70% the modulus of elasticity of the intact body [9]. The parametric study was performed for E values between 20 GPa and 63.79 GPa. The analysis yielded significant influence for the E value on the modal frequency results (Figure 6). The modal frequencies of the first 11 modes of vibration presented an increase between 0.82% and 2.36% per GPa (Table 3). The value of E yielded zero influence on the effective mass distribution over the modes. Moreover, the qualitative results of the modes of vibration, i.e. order of modes and modal shapes, were similarly not affected by the variation of the E parameter.

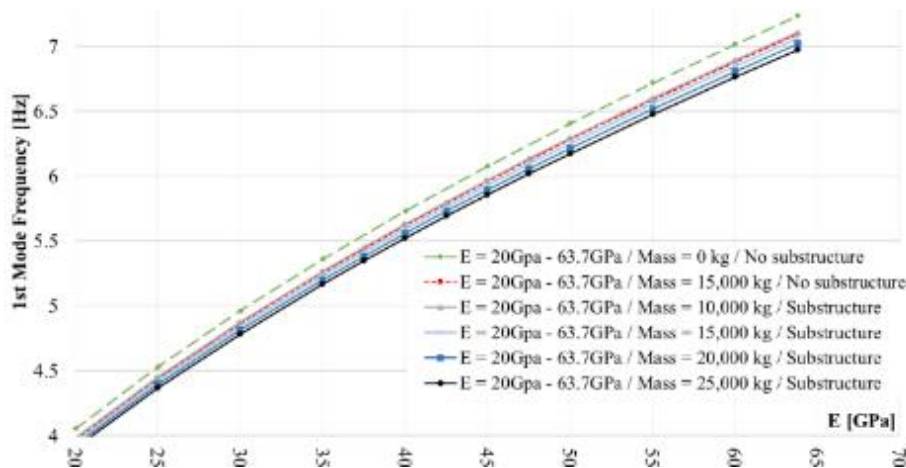


Figure 6: Parametric analysis results of the influence of E , added mass and substructure on the frequency values of the 1st mode of vibration.

5.4 Added mass on the top

For studying the influence of the non-structural mass on the top of the lighthouse, mass values between 0 kg and 25000 kg were considered. The analysis results and the influence of this mass on the numerical outputs is shown in Figure 6 and Table 3. The results revealed a slight decrease of the modal frequency values that ranges between -0.07% and -0.13% per 1000 kg of added mass. However, this non-structural mass did not affect the direction of oscillation of the first 4 modes of vibration. On the other hand, a moderate influence was found for the effective masses which for the first 4 modes were found differentiated between -0.20% to 3.50%.

5.5 Synopsis of parametric analysis

The parametric study quantified the influence of the analysed parameters (Element type, Substructure, E , added mass) on the dynamic analysis results (f , φ , m^*). The level of influence for each input-output couple is presented in Table 3 and Table 4.

Table 3: Quantified influence of the parameters on the modal results

Parameter	Modal frequency $\Delta f/f$	Direction of oscillation $\Delta\phi$	Effective mass $\Delta m^*/m^*$
Element type	-0.20% to 0.20% if changed	0° if changed	-3.27% to 5.82% if changed
Substructure	-0.40% to -0.98% if modelled	-4.18% to 3.45% if modelled	-21.2% to 17.1% if modelled
E increase	0.82% to 2.36% /GPa	$\approx 0^\circ$ /GPa	0 /GPa
Added mass	-0.07% to -0.13% /1000 kg	$\approx 0^\circ$ /1000 kg	-0.02% to 0.35% /1000 kg

Table 4: Influence of the parameters on the modal results

Parameter	Modal frequency $\Delta f/f$	Direction of oscillation $\Delta\phi$	Effective mass $\Delta m^*/m^*$
Element type	Slight	None	Moderate
Substructure	Slight	Moderate	Heavy
E	Heavy	None	None
Added mass	Slight	None	Moderate

The modulus of elasticity was proved the most influence parameter in terms of modal frequency results. Therefore, a proper calibration of the numerical model should focus on the correct estimation of the E parameter. As an example of its importance, a 20 GPa increase of E can cause up to 47.2% of increase in some modal frequencies (Table 5).

Table 5: Magnitude of variation of the modal results due to changes of the input parameters

Variation of input parameters		Variation of output results		
Parameter		Modal frequency $\Delta f/f$	Direction of oscillation $\Delta\phi$	Effective mass $\Delta m^*/m^*$
Change element type	True	-0.20% to 0.20%	0°	-3.27% to 5.82%
Substructure modelled	True	-0.40% to -0.98%	-4.18% to 3.45%	-21.2% to 17.1%
E increased by	20 GPa	16.4% to 47.2%	$\approx 0^\circ$	0
Added mass of	10000 kg	-0.70% to -1.30%	$\approx 0^\circ$	-0.20% to 3.50%

The non-structural mass slightly reduced the frequency values and moderately influenced the effective mass distribution. Therefore, although considering a non-structural mass of the top for simulating the weight of the lightning apparatus and pedestal is indeed important, since its influence is not crucial, calculating this mass with precision is of secondary importance. For instance, a variation of 10000 kg could cause a decrease of up to -1.30% in f values and a variation of m^* values of up to 3.50% (Table 5).

The substructure was found to affect the frequency values slightly, the direction of oscillation moderately and the effective masses heavily. Therefore, if the volume of the substructure is not negligible compared to the rest of the structure, it is highly recommended to model this part.

6. CALIBRATION OF THE FE MODEL

The final calibration of the numerical model was performed with the use of the expensive C3D20 finite elements. As Table 6 and Figure 7 present, a very good fit was achieved between the experimental dynamic identification and the FEM results. The results presented in Table 6 were obtained using a modulus of elasticity E equal to 30 GPa and 15,000 kg of non-structural

mass on the top. This E value corresponds to the 47% of the value found in bibliography for the intact granite material. The same value corresponds to a range of 69% to 91 % of the values yielded by the Schmidt hammer testing. Moreover, the testing campaign revealed that the lighthouse has slightly higher modal frequencies in one of the two directions for the first two pairs of modes. To simulate this, lateral uniaxial displacement constrains were added to the model at the area near the entrance door where the lateral rock is in contact with the structure.

Table 6: Comparison of modal frequency values between FEM and experimental results

	1 st mode	2 nd mode	3 rd mode	4 th mode
FEM	4.84 Hz	5.16 Hz	17.41 Hz	19.70 Hz
Experimental	4.82 Hz	5.18 Hz	18.50 Hz	19.10 Hz

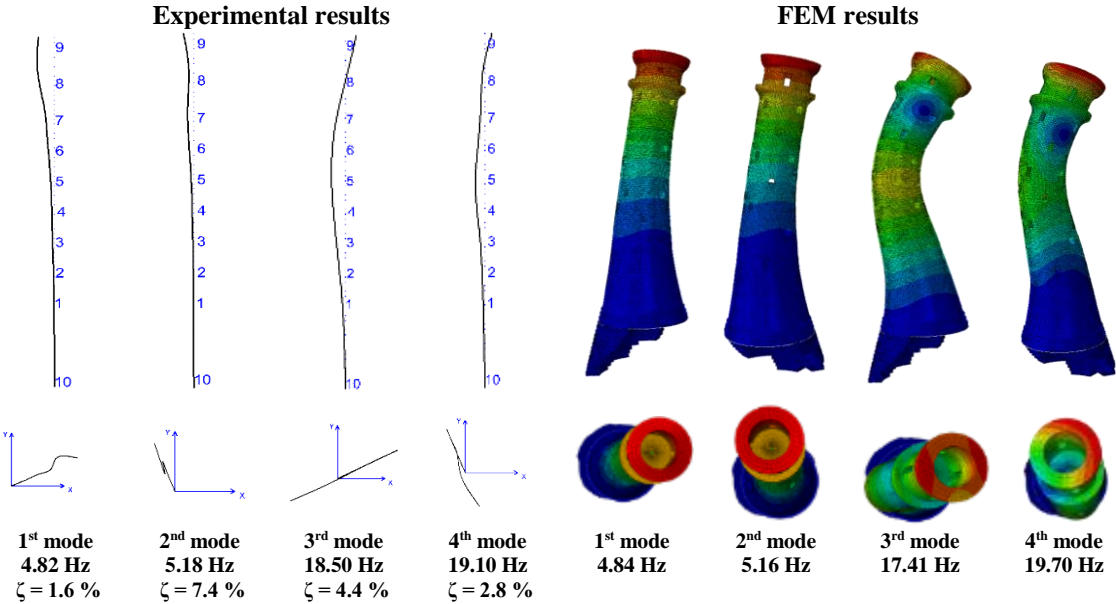


Figure 7: Modal frequencies and shapes for Fastnet lighthouse, experimental results from ambient data (left); FEM results with Young’s modulus $E= 30$ GPa, added mass $M=15,000$ kg, modelled substructure and uniaxial lateral constraints (right).

7. CONCLUSIONS

This paper presents a summary of the work needed for creating and calibrating a FEM model of a tapered lighthouse structure. Detailed bibliographic information and original architectural drawings allowed the creation of an accurate model geometry. Thanks to this data, uncertainties regarding the material self-weight and dimensions are eliminated. A parametric analysis reveals that the existence of the substructure has a strong influence on the modal mass results (i.e. between -21.2% and 17.1%). Moreover, a moderate influence on the effective masses is found for the finite element type (i.e. up to 5.82%) and the added mass on the top (i.e. up to 0.35% per 1000 kg). The direction of oscillation depends moderately on the existence of the substructure and heavily on the imposition of lateral constrains due to the contact of the structure with the adjacent rock mass. The modal frequency results are found to be heavily dependent on the value of the modulus of elasticity (i.e. up to 2.36% per GPa).

Given the close correlation between the E values and modal frequencies, the calibration of the FE model is mainly focused on this parameter. The demanding on-site experimental campaign produced valuable results for making the calibration possible. A very good fit between experimental and numerical values is achieved both in terms of modal shapes and frequencies. The E value that is adopted for the calibrated model (i.e. 30 GPa) corresponds to a significantly lower value than the one estimated for the intact granite material (i.e. 47% of the bibliography estimated value and 69% to 91% of the Schmidt hammer test estimated value). The interaction of the structure with the lateral rock mass, which had not been considered before the on-site work, was identified both by visual inspection and the experimental results that revealed higher stiffness in one direction for the lower modes.

The present calibrated model will be used for thorough non-linear analysis for investigating the impact effect of extreme sea waves on the Fastnet lighthouse. The experience obtained by this coupled experimental and numerical work will be used for studying the rest of the historic lighthouses included in the STORMLAMP project and can become point of reference for works on other historic lighthouses or similar structures.

ACKNOWLEDGMENTS

The authors would like to thank the UK Engineering and Physical Sciences Research Council (EPSRC) for the financial support of the STORMLAMP project EP/N022947/1 and the Irish Lights for the provision of detailed drawings and for physical access to the Fastnet lighthouse.

REFERENCES

- [1] Morrissey, J., 'A history of the Fastnet lighthouse', 2nd Edn. (Crannog Books, Dublin 2005).
- [2] Watson, J., 'British and foreign building stones'. (Cambridge University Press, Cambridge 1911).
- [3] Abaqus, 'Abaqus documentation - version 6.14, Dassault Systèmes, Providence, RI, USA.' (2014).
- [4] Brownjohn, J., Raby, A., Bassitt, J., Hudson, E., and Antonini, A., 'Modal testing of offshore rock lighthouses around the British Isles', Proceedings of the 10th international conference on structural dynamics EUROLYN, (2017).
- [5] Katz, O., Reches, Z., and Roegiers, J.C., 'Evaluation of mechanical rock properties using a Schmidt hammer', *Int. J. rock Mech. Min. Sci.* **37** (2000) 723-728.
- [6] Sumner, P. and Nel, W., 'The effect of rock moisture on Schmidt hammer rebound: tests on rock samples from Marion Island and South Africa', *Earth Surf. Process. Landforms* **27**, (2002) 1137–1142.
- [7] Aydin, A. and Basu, A., 'The Schmidt hammer in rock material characterization', *Eng. Geol.* **81** (2005) 1-14.
- [8] Vasconcelos, G., Lourenço, P.B., Alves, C.S.A., and Pamplona, J., 'Prediction of the mechanical properties of granites by ultrasonic pulse velocity and Schmidt hammer hardness', in 10th North American masonry conference, (2007) 998–1009.
- [9] Min, K.B. and Jing, L., 'Numerical determination of the equivalent elastic compliance tensor for fractured rock masses using the distinct element method', *Int. J. Rock Mech. Min. Sci.* **40** (2003) 795–816.